

Protoneutron stars in the Brueckner-Hartree-Fock approach and finite-temperature kaon condensation

A. Li (李昂) and X. R. Zhou (周先荣)

Institute of Theoretical Physics and Astrophysics, Department of Physics, Xiamen University, Xiamen 361005, P. R. China

G. F. Burgio and H.-J. Schulze

INFN, Sezione di Catania, Via Santa Sofia 64, I-95123 Catania, Italy

We study the properties of hot neutrino-trapped β -stable stellar matter using an equation of state of nuclear matter within the Brueckner-Hartree-Fock approach including three-body forces, combined with a standard chiral model for kaon condensation at finite temperature. The properties of (proto)neutron stars are then investigated within this framework.

PACS numbers: 26.60.Kp, 26.60.-c, 26.50.+x, 13.75.Jz, 21.65.Jk

I. INTRODUCTION

One of the challenging problems in nuclear physics is to elucidate the behavior of nuclear matter in high-density and/or high-temperature environments, particularly relevant for compact stellar objects like (proto)neutron stars [(P)NS]. Despite the importance of the structure and properties of β -stable matter at extreme densities of several times normal nuclear matter density ($\rho_0 \approx 0.17 \text{ fm}^{-3}$), its internal constitution and the equation of state (EOS) are not yet known with certainty.

At such densities strangeness may occur in the form of hadrons (such as hyperons or a K^- meson condensate) or in the form of strange quarks. The existence of these strange matter phases may have important consequences for the structure of compact stars and for the cooling dynamics of the PNS after a supernova explosion. With respect to kaons, the suggestion of Kaplan and Nelson [1] that at high enough densities the ground state of baryonic matter might contain a Bose-Einstein (BE) condensate of negatively charged kaons has prompted extensive investigations and discussions [2–17] on its implications for astrophysical phenomena in (P)NS's. In particular, the proton abundance is increased dramatically when a kaon condensate is present in NS matter, and antileptons are allowed to exist.

Some authors treated kaon condensation within an improved chiral perturbation theory beyond the tree-order calculations, and their results indicated that the critical density ρ_c^K for kaon condensation lies in the range of $2\rho_0 \lesssim \rho_c^K \lesssim 4\rho_0$. The critical density depends sensitively on the value of the strangeness content of the proton, which is still quite controversial [5, 8, 15, 18–22].

Estimates of the relevant formation timescales [3, 10] indicate that the build-up of the kaon condensate is very fast compared to the typical cooling and neutrino-diffusion timescale of several seconds characteristic for a PNS, and could even play a role during the preceding supernova core collapse. Therefore, a kaon condensate might be present immediately after the formation of a PNS, and influence its evolutionary history. In fact, lepton trapping in a PNS shifts the onset of kaon condensation to higher densities as compared to neutrino-free matter. Also the presence of other strange particles (for instance, hyperons) was found to push the onset of

kaon condensation to higher densities, even out of the physically relevant density regime, $\rho \lesssim 1 \text{ fm}^{-3}$, [8, 23]. This leads to the widely discussed possibility of a delayed collapse of the PNS to a black hole, when during the cooling and deleptonization evolution the increasing softening effect of the kaons on the EOS becomes too big to stabilize an initially very massive star [4, 8, 9, 11, 24].

Obviously, for a reliable modeling of this effect both conditions of finite temperature and lepton trapping have to be taken into account. However, most of the previous investigations have been done for cold matter, thus neglecting the dependence of the kaon condensation on temperature, which plays a role in affecting significantly the properties of PNS's [25–28]. Therefore we extend our previous work [16, 17] to hot matter. The main goal of this article is to investigate the impact of a kaon condensate on PNS matter at finite temperature and on the final PNS observables, combining a microscopic Brueckner-Hartree-Fock (BHF) approach for the baryonic part of the matter with a standard chiral model for the kaon-nucleon contribution.

Our paper is organized as follows. In Sec. IIA we discuss the finite-temperature BHF approach, and in Sec. IIB the standard chiral model at finite temperature. The composition of stellar matter and the EOS are presented in Sec. III, along with the equations of stellar structure. The numerical results are then illustrated in Sec. IV, and conclusions are drawn in Sec. V.

II. THEORETICAL MODELS

In the kaon-condensed phase of (P)NS matter, the free energy density consists of three contributions,

$$f = f_{NN} + f_{KN} + f_L, \quad (1)$$

where f_{NN} is the baryonic part, f_{KN} is the kaonic part including the contribution from the kaon-nucleon interaction, and f_L denotes the contribution of leptons e, μ, ν_e, ν_μ , and their antiparticles.

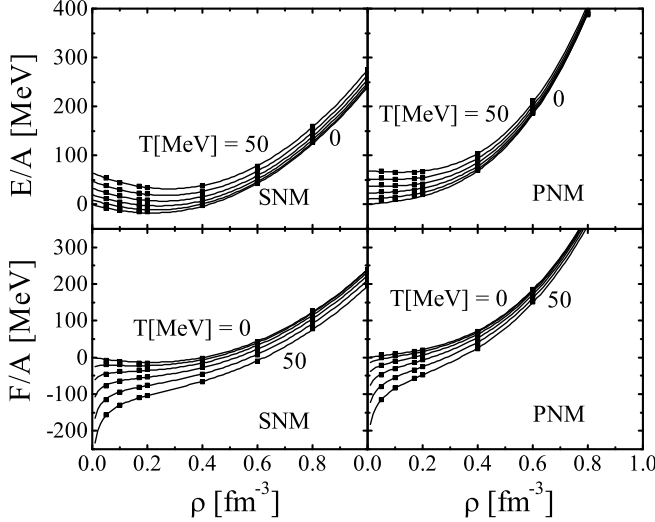


FIG. 1: Finite-temperature EOS for symmetric (left panels) and purely neutron (right panels) matter. The internal energy (upper panels) and the free energy (lower panels) are displayed as a function of the nucleon density, for temperatures ranging from 0 to 50 MeV in steps of 10 MeV. The numerical data (markers) and the results of the fits, Eqs. (10,11), (curves) are shown.

A. Brueckner-Bethe-Goldstone theory at finite temperature

In the present work, we employ the BHF approach for asymmetric nuclear matter at finite temperature [27, 29–32] to calculate the baryonic contribution to the EOS of stellar matter. The essential ingredient of this approach is the interaction matrix G , which satisfies the self-consistent equations

$$G(\rho, x; E) = V + V \sum_{1,2} \frac{|12\rangle(1-n_1)(1-n_2)\langle 12|}{E - e_1 - e_2 + i0} G(\rho, x; E) \quad (2)$$

and

$$U_1(\rho, x) = \text{Re} \sum_2 n_2 \langle 12 | G(\rho, x; e_1 + e_2) | 12 \rangle_a, \quad (3)$$

where $x = \rho_p/\rho$ is the proton fraction, and ρ_p and ρ are the proton and the total baryon density, respectively. E is the starting energy and $e(k) \equiv k^2/2m + U(k)$ is the single-particle (s.p.) energy. The multi-indices 1,2 denote in general momentum, isospin, and spin.

The realistic nucleon-nucleon (NN) interaction V adopted in the present calculation is the Argonne V_{18} two-body force [33] supplemented by either a microscopic three-body force (TBF) based on the meson-exchange approach [34–36] (denoted micro TBF in the following), or the phenomenological Urbana UIX force discussed in Refs. [37, 38] (pheno TBF), which are reduced to an effective two-body force and added to the bare potential in the BHF calculation (see Refs. [34–36] for details).

At finite temperature, $n(k)$ in Eqs. (2) and (3) is a Fermi distribution. For a given density and temperature, these equations have to be solved self-consistently along with the following

equations for the auxiliary chemical potentials $\tilde{\mu}_{n,p}$,

$$\rho_i = 2 \sum_k n_i(k) = 2 \sum_k \left[\exp\left(\frac{e_i(k) - \tilde{\mu}_i}{T}\right) + 1 \right]^{-1}. \quad (4)$$

To save computational time and simplify the numerical procedure, in the following we employ the so-called *Frozen Correlations Approximation* [27, 32], i.e., the correlations at $T \neq 0$ are assumed to be essentially the same as at $T = 0$. This means that the s.p. potential $U_i(k)$ for the component i at finite temperature is approximated by the one calculated at $T = 0$. Within this approximation, the nucleonic free energy density has the following simplified expression,

$$f_{NN} = \sum_{i=n,p} \left[2 \sum_k n_i(k) \left(\frac{k^2}{2m_i} + \frac{1}{2} U_i(k) \right) - T s_i \right], \quad (5)$$

where

$$s_i = -2 \sum_k \left(n_i(k) \ln n_i(k) + [1 - n_i(k)] \ln [1 - n_i(k)] \right) \quad (6)$$

is the entropy density for the component i treated as a free Fermi gas with spectrum $e_i(k)$. It turns out that the assumed independence is valid to a good accuracy [27, 32], at least for not too high temperature, $T \lesssim 30$ MeV.

For illustration, we display in Fig. 1 the EOS obtained following the above discussed procedure, for symmetric nuclear matter and purely neutron matter, adopting the micro TBF. In the upper panels we display the internal energy per particle, whereas the lower panels show the free energy as a function of the baryon density, for several values of temperature between 0 and 50 MeV. We notice that the free energy of symmetric matter is a monotonically decreasing function of temperature. At $T = 0$ the free energy coincides with the internal energy and the corresponding curve is just the usual nuclear matter saturation curve. On the contrary, the internal energy is an increasing function of temperature. The effect is less pronounced for pure neutron matter due to the larger Fermi energy of the neutrons at given density. We notice that the results of this microscopic TBF are always stiffer than those of the phenomenological Urbana TBF [37] used in Ref. [38].

For practical use, we provide analytical fits of the internal energy $E/A(T, \rho, x)$ as well as the free energy $F/A(T, \rho, x)$. It turns out that for both quantities the dependence on proton fraction can be very well approximated by a quadratic dependence, as at zero temperature [30, 39]:

$$\frac{E}{A}(T, \rho, x) \approx \frac{E}{A}(T, \rho, x=0.5) + (1-2x)^2 E_{\text{sym}}(T, \rho), \quad (7)$$

where the symmetry energy E_{sym} can be expressed in terms of the difference of the energy per particle between pure neutron ($x=0$) and symmetric ($x=0.5$) matter:

$$\begin{aligned} E_{\text{sym}}(T, \rho) &= -\frac{1}{4} \frac{\partial(E/A)}{\partial x}(T, \rho, 0) \\ &\approx \frac{E}{A}(T, \rho, 0) - \frac{E}{A}(T, \rho, 0.5). \end{aligned} \quad (8)$$

TABLE I: Parameters of the EOS fits, Eqs. (10,11), for symmetric nuclear matter (SNM) and pure neutron matter (PNM) and both nuclear TBF's used.

micro TBF	a_1	a_2	b_0	b_1	b_2	c_0	c_1	d
E/A , SNM	81	95	-155	-139		395	81	2.09
E/A , PNM	101	73	54	-181		659	84	2.88
F/A , SNM	41	120	-115		-182	355		2.24
F/A , PNM	18	123	83		-103	631		3.02
pheno TBF	a_1	a_2	b_0	b_1	b_2	c_0	c_1	d
E/A , SNM	105	74	-473	-464		586	381	1.26
E/A , PNM	109	64	34	-240		249	164	1.97
F/A , SNM	41	116	-180		-174	293		1.57
F/A , PNM	21	116	101		-131	191		2.62

Therefore, it is only necessary to provide parametrizations of both quantities for symmetric nuclear matter and pure neutron matter. We find that the following functional forms provide excellent parametrizations of the numerical results in the required ranges of density ($0.03 \text{ fm}^{-3} \lesssim \rho \lesssim 1 \text{ fm}^{-3}$) and temperature ($0 \text{ MeV} \leq T \leq 50 \text{ MeV}$):

$$\begin{aligned} \frac{E}{A}(\rho, T) &= (a_1 t + a_2 t^2) + (b_0 + b_1 t)\rho + (c_0 + c_1 t)\rho^d, (10) \\ \frac{F}{A}(\rho, T) &= (a_1 t + a_2 t^2) \ln(\rho) + (b_0 + b_2 t^2)\rho + c_0 \rho^d, (11) \end{aligned}$$

where $t = T/(100 \text{ MeV})$ and E, F , and ρ are given in MeV and fm^{-3} , respectively. The parameters of the different fits are given in Table I for both TBF's we are using.

B. Kaon condensate at finite temperature

Kaon condensation in nuclear matter has been studied intensively in a large variety of models. For the required extension to finite temperature we employ the formalism of Refs. [9, 10], which treats fluctuations around the condensate within the framework of chiral symmetry. For small condensate amplitudes this approach is exactly equivalent to the meson-exchange mean-field models of Ref. [11], and we briefly review it now.

In the following equations, m_K and μ_K are the kaon mass and chemical potential, $f_\pi = 93 \text{ MeV}$ is the pion decay constant, θ is the amplitude of the condensate,

$$E_p^\pm = \sqrt{p^2 + \tilde{m}_K^2} \pm \tilde{\mu}_K \quad (12)$$

are the kaonic excitation energies [5, 9, 11, 15] with

$$\tilde{m}_K = \sqrt{m_K^{*2} \cos^2 \theta + b^2}, \quad (13)$$

$$\tilde{\mu}_K = \mu_K \cos \theta + b, \quad (14)$$

and

$$m_K^{*2} = m_K^2 + (a_1 x + a_2 + 2a_3) m_s \rho / f_\pi^2, \quad (15)$$

$$b = (1+x)\rho / 4f_\pi^2 \quad (16)$$

are the scalar effective kaon mass and the V -spin density, respectively.

We adopt the 'standard' KN interaction parameters [2, 5, 8, 9, 15] $a_1 m_s = -67 \text{ MeV}$, $a_2 m_s = 134 \text{ MeV}$, and $a_3 m_s = -134, -222, -310 \text{ MeV}$ to perform our numerical calculations, where the different choices of a_3 correspond to different values of the strangeness content of the proton, $y = 2\langle p|\bar{s}s|p\rangle/\langle p|\bar{u}u + \bar{d}d|p\rangle \approx 0, 0.36[19], 0.5[20]$, in the chiral model.

We remark that the most recent lattice determination of the strangeness content of the proton [22] (as well as recent theoretical results [21]) indicate a very low value $y < 0.05$, in strong disagreement with previous calculations [18–20]. If confirmed, such a small value would imply also a very small absolute value of a_3 . Using [5] $\langle p|\bar{d}d|p\rangle \approx \langle p|\bar{u}u|p\rangle = -(a_1 + 2a_3)$ and $\langle p|\bar{s}s|p\rangle = -2(a_2 + a_3)$ we obtain

$$a_3 \approx \frac{a_1 y / 2 - a_2}{1 - y} \gtrsim \frac{-143 \text{ MeV}}{m_s}, \quad (17)$$

and kaon condensation would be strongly disfavored in the present model, as will be illustrated below.

The thermodynamic potential densities due to the condensed kaons and the thermal kaons are introduced as follows:

$$\omega_{KN}^c = f_\pi^2 \left[(m_K^{*2} - 2b\mu_K)(1 - \cos \theta) - \mu_K^2 \frac{\sin^2 \theta}{2} \right], \quad (18)$$

$$\omega_{KN}^{\text{th}} = T \int \frac{d^3 p}{(2\pi)^3} \ln \left[(1 - e^{-\beta E_p^+})(1 - e^{-\beta E_p^-}) \right]. \quad (19)$$

Then the kaonic (charge) density q_K is given by

$$\begin{aligned} q_K &= -\frac{\partial \omega_{KN}}{\partial \mu_K} \\ &= f_\pi^2 \left[2b(1 - \cos \theta) + \mu_K \sin^2 \theta \right] \\ &\quad + \cos \theta \int \frac{d^3 p}{(2\pi)^3} \left[f_B(E_p^-) - f_B(E_p^+) \right], \quad (21) \end{aligned}$$

where the last term is the contribution due to thermally excited kaons, q_K^{th} , with the Bose distribution function $f_B(E) = 1/(e^{\beta E} - 1)$.

The kaon-nucleon free energy density appearing in Eq. (1) obtained in this way is

$$f_{KN} = \omega_{KN} + \mu_K q_K \quad (22)$$

$$\begin{aligned} &= f_\pi^2 \left[m_K^{*2} (1 - \cos \theta) + \mu_K^2 \frac{\sin^2 \theta}{2} \right] \\ &\quad + \mu_K q_K^{\text{th}} + \omega_{KN}^{\text{th}}, \quad (23) \end{aligned}$$

and the internal energy density is

$$\varepsilon_{KN} = f_{KN} + T s_K, \quad (24)$$

where the kaonic entropy density is solely due to the thermal kaons:

$$s_K = -\frac{\partial \omega_{KN}}{\partial T} = \beta \left(\varepsilon_{KN}^{\text{th}} - \omega_{KN}^{\text{th}} \right) \quad (25)$$

with

$$\varepsilon_{KN}^{\text{th}} = \int \frac{d^3p}{(2\pi)^3} \left[E_p^- f_B(E_p^-) + E_p^+ f_B(E_p^+) \right]. \quad (26)$$

One can determine the ground state by minimizing the total grand-canonical potential density ω_{KN} with respect to the condensate amplitude θ , keeping (μ_K, ρ, x) fixed. This minimization together with the chemical equilibrium and charge neutrality conditions leads to the following three coupled equations [5, 9, 15]

$$0 = f_\pi^2 \sin \theta \left[m_K^{*2} - 2b\mu_K - \mu_K^2 \cos \theta \right] + \frac{\partial \omega_{KN}^{\text{th}}}{\partial \theta}, \quad (27)$$

$$\begin{aligned} \mu_K &= \mu_n - \mu_p \\ &= 4(1-2x) \frac{F_{\text{sym}}}{A} - (a_1 m_s - \mu_K/2)(1 - \cos \theta) \\ &\quad - \frac{1}{\rho} \frac{\partial \omega_{KN}^{\text{th}}}{\partial x}, \end{aligned} \quad (28)$$

$$q_K + q_e + q_\mu = q_p = x\rho. \quad (29)$$

Note that neglecting the thermal contribution in Eq. (27) implies $\tilde{\mu} = \tilde{m}$ and therefore $E_0^- = 0$ in Eqs. (12–14), consistent with a singularity of the BE distribution function and the existence of the condensate. We therefore neglect also the thermal contribution in Eq. (28), as is done in Ref. [9].

The lepton number density is given by ($l = e, \mu, \nu$):

$$q_l = g_l \int \frac{d^3p}{(2\pi)^3} \left[f_F(e_l(\mathbf{p}) - \mu_l) - f_F(e_l(\mathbf{p}) + \mu_l) \right] \quad (30)$$

with the Fermi distribution function $f_F(E) = 1/(e^{\beta E} + 1)$, $e_l(\mathbf{p}) = \sqrt{m_l^2 + p^2}$, and the degeneracies $g_e = g_\mu = 2$, $g_\nu = 1$.

The composition and the EOS of the kaon-condensed phase in the chemically equilibrated (P)NS matter can be obtained by solving the coupled equations (27), (28), and (29). The critical density for kaon condensation is determined as the point above which a real solution with $\theta > 0$ for the coupled equations can be found.

III. COMPOSITION AND EOS OF HOT STELLAR MATTER

In neutrino-trapped β -stable nuclear matter the chemical potential of any particle $i = n, p, K, l$ is uniquely determined by the conserved quantities baryon number B_i , electric charge Q_i , and weak charges (lepton numbers) $L_i^{(e)}, L_i^{(\mu)}$:

$$\mu_i = B_i \mu_n - Q_i \mu_K + L_i^{(e)} \mu_{\nu_e} + L_i^{(\mu)} \mu_{\nu_\mu}. \quad (31)$$

For stellar matter containing nucleons, kaons, and leptons as relevant degrees of freedom, the chemical equilibrium conditions read explicitly

$$\mu_K = \mu_n - \mu_p = \mu_e - \mu_{\nu_e} = \mu_\mu + \mu_{\nu_\mu}. \quad (32)$$

At given baryon density ρ , these equations have to be solved together with the charge neutrality condition

$$\sum_i Q_i x_i = 0 \quad (33)$$

and those expressing conservation of lepton numbers

$$Y_l = x_l - x_{\bar{l}} + x_{\nu_l} - x_{\bar{\nu}_l}, \quad l = e, \mu. \quad (34)$$

Gravitational collapse calculations of the electron-degenerate core of massive stars indicate that at the onset of trapping, the electron lepton number is $Y_e = x_e + x_{\nu_e} \approx 0.4$, the precise value depending on the efficiency of electron capture reactions during the initial collapse stage. Also, because no muons are present when neutrinos become trapped, the constraint $Y_\mu = x_\mu - x_{\bar{\nu}_\mu} = 0$ is imposed. We fix the Y_l at these values in our calculations for neutrino-trapped matter. When the neutrinos have left the system, their partial densities and chemical potentials vanish and the above equations simplify accordingly.

The various chemical potentials are obtained from the total free energy density f , Eq. (1),

$$\mu_i(\{\rho_j\}) = \left. \frac{\partial f}{\partial \rho_i} \right|_{\rho_{j \neq i}}. \quad (35)$$

Once the hadronic and leptonic chemical potentials are known, one can proceed to calculate the composition of the β -stable stellar matter, and then the total pressure p through the usual thermodynamical relation

$$p = \rho^2 \frac{\partial (f/\rho)}{\partial \rho} = \sum_i \mu_i \rho_i - f. \quad (36)$$

The stable configurations of a (P)NS can be obtained from the well-known hydrostatic equilibrium equations of Tolman, Oppenheimer, and Volkov [40] for pressure $p(r)$ and enclosed mass $m(r)$

$$\frac{dp}{dr} = - \frac{Gm\varepsilon}{r^2} \frac{(1+p/\varepsilon)(1+4\pi r^3 p/m)}{1-2Gm/r}, \quad (37)$$

$$\frac{dm}{dr} = 4\pi r^2 \varepsilon, \quad (38)$$

once the EOS $p(\varepsilon)$ is specified, with $\varepsilon = \varepsilon_{NN} + \varepsilon_{KN} + \varepsilon_L$ the total internal energy density (G is the gravitational constant). For a chosen central value of the energy density, the numerical integration of Eqs. (37) and (38) provides the mass-radius relation.

Dynamical simulations of supernovae explosions [11, 41, 42] show that the PNS has neither an isentropic nor an isothermal profile. For simplicity we assume a constant temperature inside the star and attach for the outer part a cold crust given in Ref. [43] for the medium-density regime ($0.001 \text{ fm}^{-3} < \rho < 0.08 \text{ fm}^{-3}$), and in Refs. [44, 45] for the outer crust ($\rho < 0.001 \text{ fm}^{-3}$). This schematizes the temperature profile of the PNS. The other extreme choice of isentropic profiles has recently been investigated within our approach [28] and no significant qualitative differences have been found.

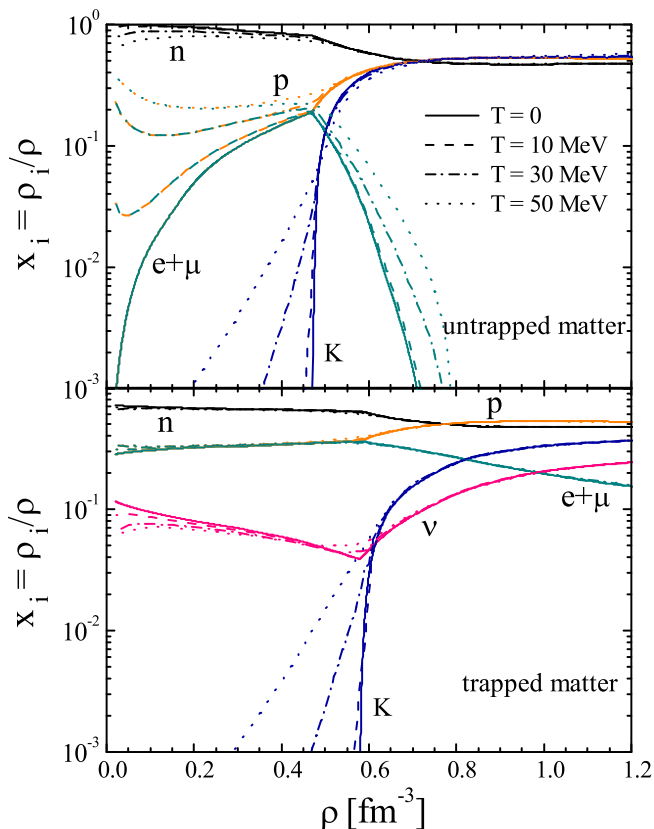


FIG. 2: (Color online) Particle fractions as a function of the baryon density in trapped ($Y_e = 0.4$, lower panel) and untrapped ($x_\nu = 0$, upper panel) β -stable matter at the temperatures $T = 0, 10, 30,$ and 50 MeV for $a_3 m_s = -222$ MeV and the micro TBF.

More realistic temperature profiles can be obtained by modeling the neutrinosphere both in the interior and in the external outer envelope, which is expected to be much cooler. A proper treatment of the transition from the hot interior to the cold outer part can have a dramatic influence on the mass – central density relation in the region of low central density and low stellar masses. In particular, the “minimal mass” region, typical of cold NS’s [40], can be shifted in PNS’s to much higher values of central density and masses. A detailed analysis of this point can be found in [46], where a model of the transition region between the interior and the external envelope is developed. However, the maximum mass region that we are interested in, is hardly affected by the structure of this low-density transition region [27].

IV. RESULTS

In the following we present the results of our numerical calculations regarding the composition of PNS matter and the structure of PNS’s.

A. Composition of stellar matter

In Fig. 2 we display the relative particle fractions (of neutrons, protons, kaons, electrons, muons, and neutrinos) in trapped (lower panel) and untrapped (upper panel) matter as a function of the baryon density for several values of temperature $T = 0, 10, 30,$ and 50 MeV, obtained with $a_3 m_s = -222$ MeV and the micro TBF. We notice that temperature effects influence the populations mainly in the low-density region, and only slightly at high density. Leptons are rather numerous at fairly small densities as a result of Fermi distributions at finite temperature.

The kaon condensate threshold density is only slightly dependent on the temperature, namely $0.489, 0.490, 0.492, 0.497 \text{ fm}^{-3}$ at $T = 0, 10, 30, 50$ MeV for untrapped matter, and $0.580, 0.583, 0.589, 0.629 \text{ fm}^{-3}$ for trapped matter, respectively. The temperature influence on the kaon population is very small above the condensate threshold and regards mainly the small fractions of thermal kaons present before the threshold. Above the critical density, thermal effects increase the population of protons and leptons in the untrapped case. We remark that, as usually found [5, 15], in cold untrapped matter the presence of a kaon condensate pushes the proton fraction above the threshold allowing fast URCA cooling.

There is a large difference between untrapped and trapped matter, where the kaon condensation sets in later, and the kaon concentration remains lower. The major reason is the smaller nuclear asymmetry of trapped matter, which leads according to Eq. (28) to a later kaon onset. [The direct dependence of the kaon effective mass on the nuclear asymmetry, Eq. (15), plays a minor role with the chosen interaction parameters]. In untrapped matter, the kaons replace immediately the leptons in compensating the charge of the protons; in trapped matter they cannot do that because the lepton number has to be kept fixed. Their effect is thus a moderate decrease of the charged leptons, while the neutrino population increases. Overall, their importance is substantially reduced compared to the case of untrapped matter.

The dependence of the composition on the KN interaction strength is illustrated in Fig. 3, where we display the relative particle fractions in trapped (lower panels) and untrapped matter (upper panels) at $T = 30$ MeV for the three different values of the interaction parameter a_3 that we consider. The onset density of kaon condensation depends strongly on this parameter and ranges approximately from 0.4 fm^{-3} to 0.6 fm^{-3} in untrapped matter, and from 0.45 fm^{-3} to 0.75 fm^{-3} in trapped matter. The fairly large onset densities for $a_3 m_s = -134$ MeV, corresponding to a small strangeness content of the proton, lie, however, in a region where the underlying concept of distinguishable baryons and mesons becomes doubtful, and also the simple chiral kaon-nucleon interaction would have to be extended.

Regarding the dependence of the particle concentrations on the TBF (micro or pheno) used, it was shown in the zero-temperature calculations of Ref. [17] that it is rather small, with only some slight differences at high density, where the micro TBF is stiffer than the pheno TBF. We therefore do not repeat this comparison here, but will only show the final

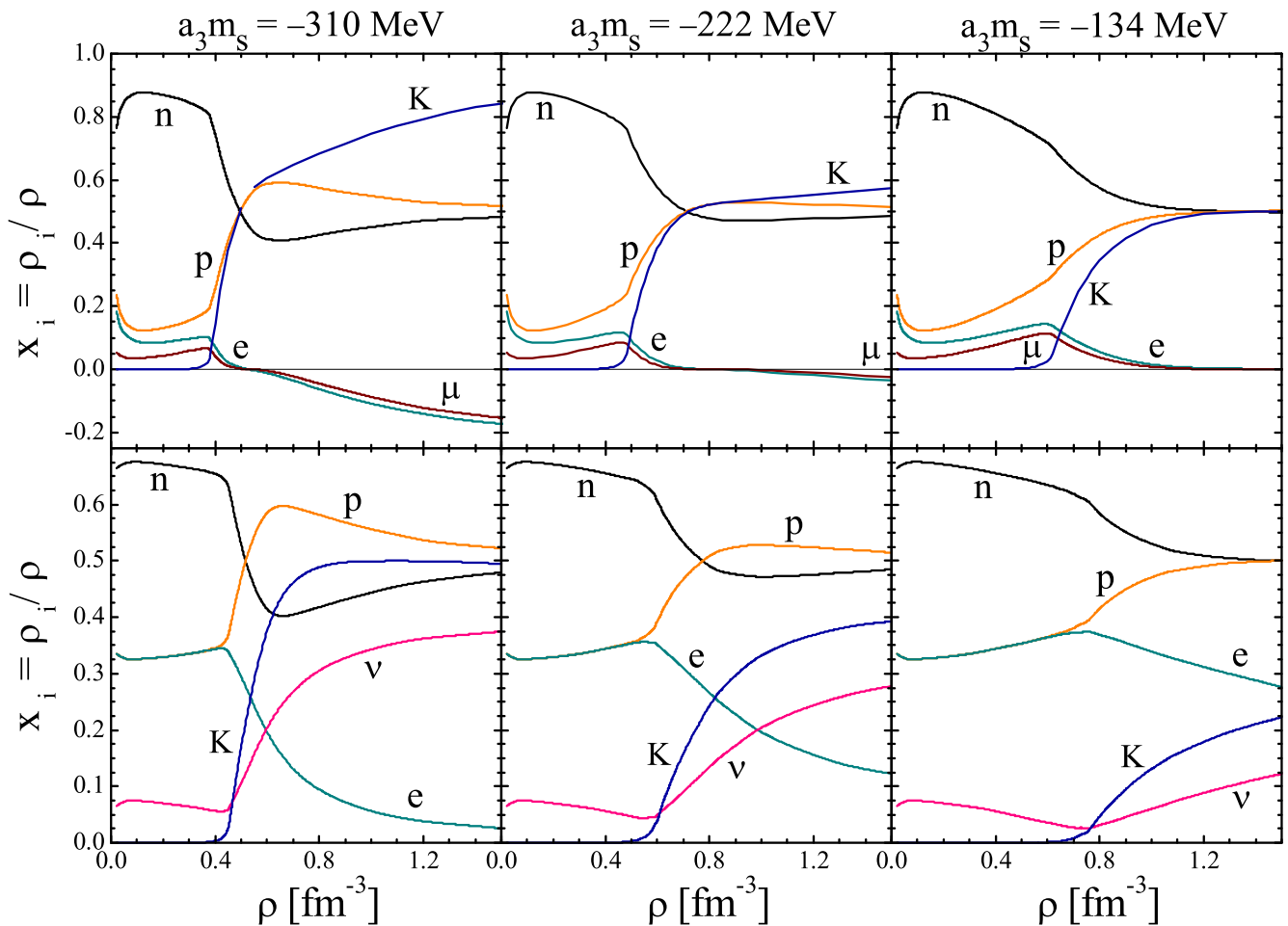


FIG. 3: (Color online) Particle fractions as a function of the baryon density in trapped ($Y_e = 0.4$, lower panels) and untrapped ($x_v = 0$, upper panels) β -stable matter, at temperature $T = 30$ MeV and with the micro TBF for $a_3m_s = -134, -222, -310$ MeV. Negative values indicate an excess of antiparticles.

(P)NS structure results obtained with both TBF's in the next subsection.

B. (Proto)neutron star structure

Fig. 4 shows the EOS $p(\rho)$ obtained with the micro TBF (upper panels) and the pheno TBF (lower panels) in the following cases: (a) no kaon condensate (left panels), (b) with kaon condensate using either $a_3m_s = -134$ MeV (middle panels) or $a_3m_s = -222$ MeV (right panels). We consider three different strongly idealized stages of the PNS evolution: (i) $T = 30$ MeV, $Y_e = 0.4$ (black dashed lines), the initial hot and neutrino-trapped state; (ii) $T = 30$ MeV, $x_v = 0$ (red dotted lines), the intermediate phase lasting about a few seconds, when most neutrinos have diffused out of the still hot environment; (iii) $T = 0$ MeV, $x_v = 0$ (green solid lines), the final state of a cold NS formed after a few tens of seconds. This rather crude treatment of the different stages of the PNS evolution can obviously be improved once more realistic temperature/trapping profiles become available. For the time being we

consider it sufficient to reflect the gross qualitative features of the important evolution stages.

We observe that the kaon condensation produces a general softening of the EOS with respect to the purely nucleonic case. The degree of softening increases with the value of the interaction parameter $|a_3m_s|$. In the case with kaon condensate, neutrino trapping produces a stiffer EOS due to the higher onset density of kaons and smaller kaon abundance, as shown in Fig. 3. This may lead a newly-formed, hot PNS to metastability, i.e., a delayed collapse while cooling down, as discussed in Refs. [8, 11]. One observes only a very small dependence of the EOS on the temperature, which plays thus a minor role in comparison with neutrino trapping. The above considerations hold true also when pheno TBF are used in the baryonic EOS (lower panels of Fig. 4), where a softer increase of the pressure vs. density is observed as compared to the case with micro TBF.

In some cases, the onset of the kaon-condensed phase produces a negative compressibility in the EOS. Following Migdal [47], we have performed a Maxwell construction to maintain a positive compressibility. This implies the forma-

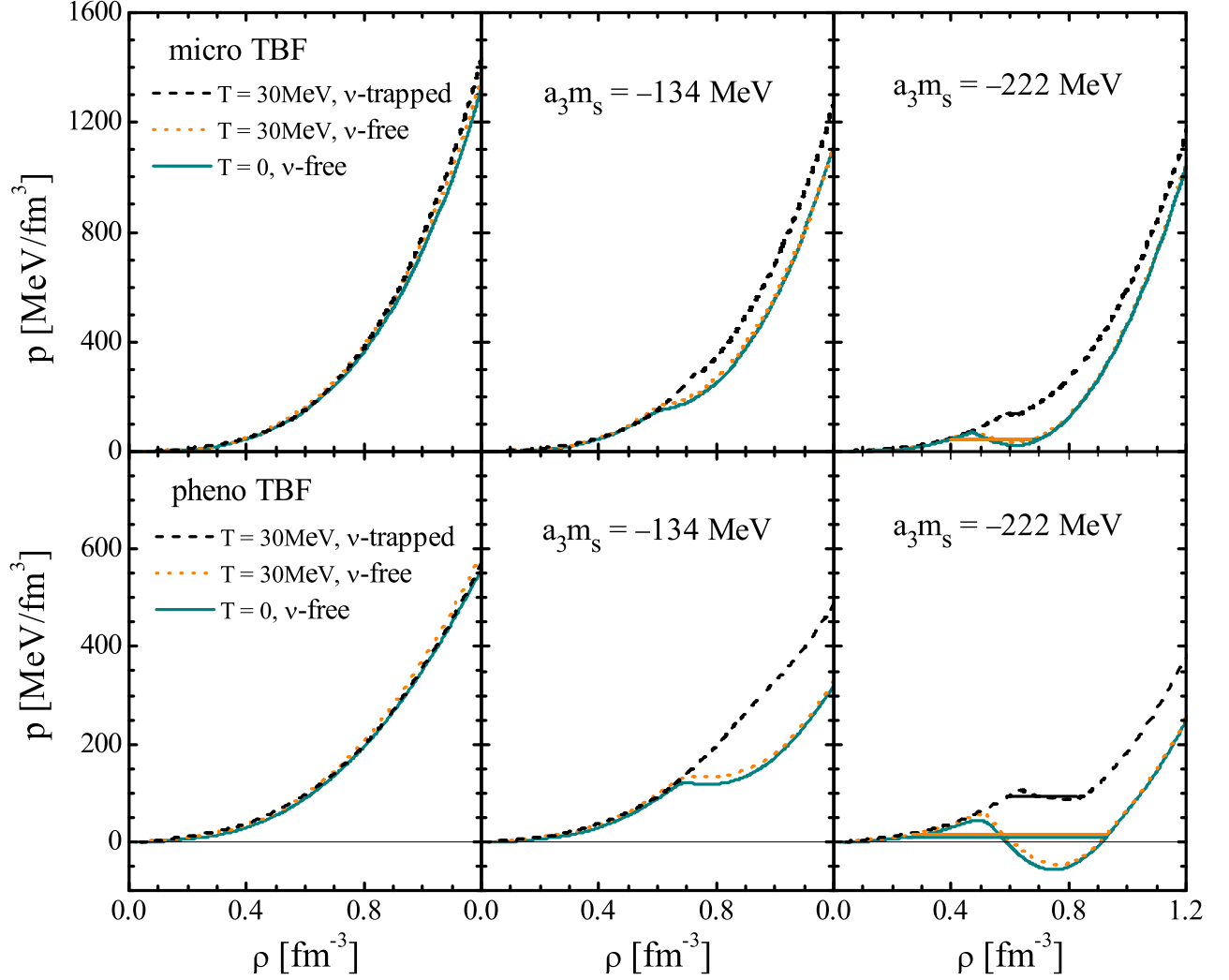


FIG. 4: (Color online) The pressure of β -stable matter under the conditions $T = 30$ MeV, $Y_e = 0.4$ (black dashed lines), $T = 30$ MeV, $x_\nu = 0$ (red dotted lines), $T = 0$ MeV, $x_\nu = 0$ (green solid lines), is shown in the following cases: no kaon condensate (left panels), with kaon condensate and $a_3 m_s = -134$ MeV (middle panels), or $a_3 m_s = -222$ MeV (left panels). The upper (lower) panels display results obtained with the micro (pheno) TBF. Horizontal line segments illustrate the Maxwell constructions.

tion of a region of constant pressure, comprised between two values of the baryon density, whose extension depends on the magnitude of $|a_3 m_s|$ [15]. It is indicated by horizontal lines in the relevant panels of Fig. 4.

These features are reflected in Fig. 5, where the corresponding gravitational mass – central density relations are plotted. The upper (lower) panels show results obtained with micro (pheno) TBF, following the same notation as in Fig. 4. In the case without kaons (left panels), the maximum mass of the PNS is slightly smaller than that of the NS, because neutrino trapping reduces the asymmetry of beta-stable matter. The presence of kaon condensation reverses the situation, and the PNS generally has a larger maximum mass than the NS, due to the less softening effect of kaons in trapped matter. A delayed collapse scenario is therefore facilitated by the presence of a kaon condensate, as is indeed generally found [5, 9, 11]. We remind that a similar effect is also produced when hyperons

are introduced in beta-stable stellar matter [27].

Again the effect of finite temperature is minor compared to the one of trapping, so that a heavy PNS would be destabilized by loss of neutrinos early during its evolution. Regarding this feature, similar conclusions as ours can be drawn from the results of Refs. [8, 9], whereas somewhat larger effects of finite temperature have been claimed in Ref. [11]. However, in that case also a higher typical temperature was assumed in stage (ii) than in stage (i) of our evolution scenario, which accounts at least for part of the observed differences. It is clearly desirable to use a more realistic temperature profile for a more reliable evaluation of this feature in the future.

A rather extreme scenario is seen in the case of a quite soft nuclear EOS combined with a strong kaon condensate (lower right panel of Fig. 5), where actually the maximum mass of the NS remains higher than that of the PNS and no delayed collapse could occur. A further consequence is the occurrence

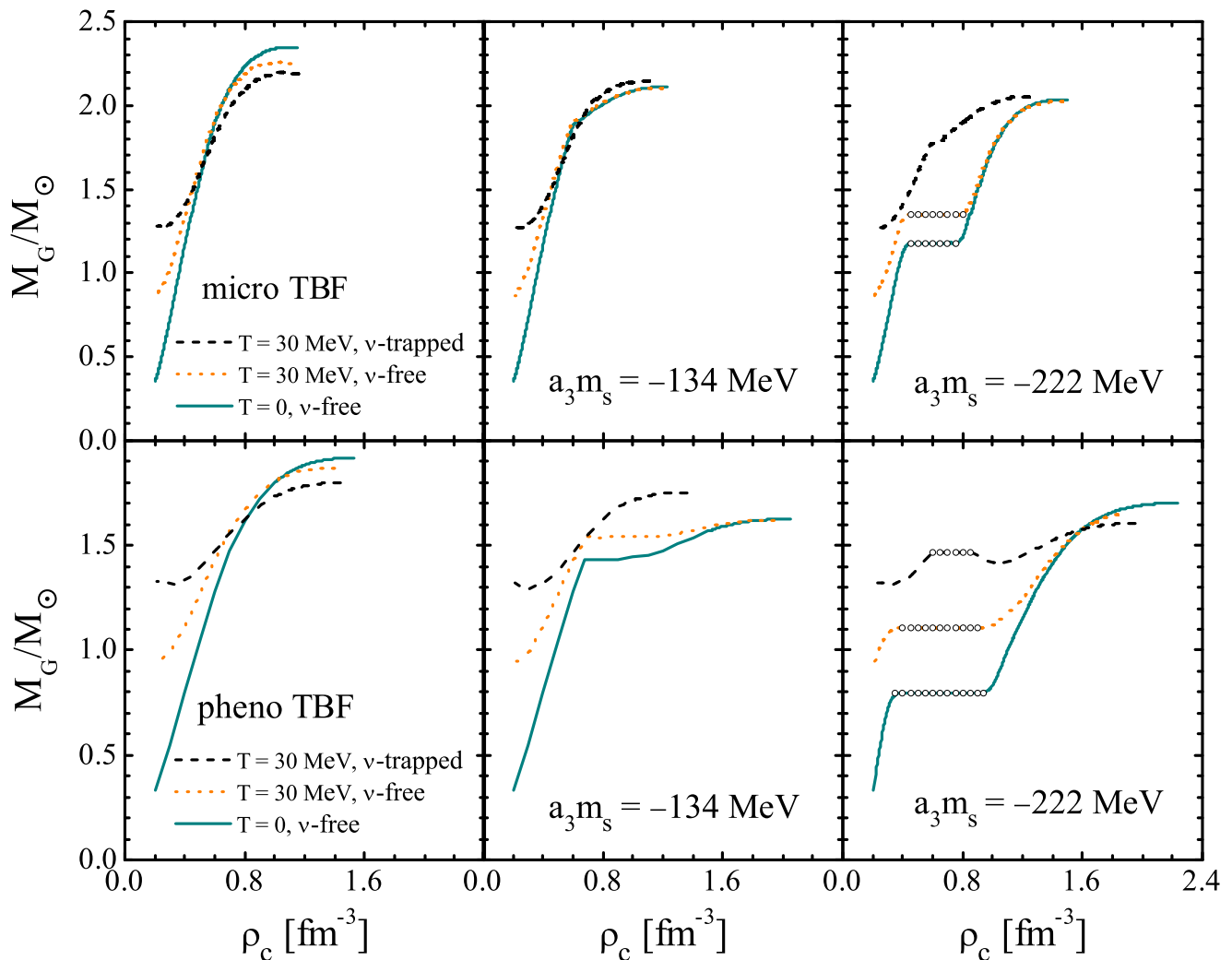


FIG. 5: (Color online) (Proto)neutron star gravitational mass – central density relations obtained with the pheno TBF (upper panels) and the micro TBF (lower panels) under the conditions $T = 30$ MeV, $Y_e = 0.4$ (black dashed lines), $T = 30$ MeV, $x_\nu = 0$ (red dotted lines), $T = 0$ MeV, $x_\nu = 0$ (green solid lines) for $a_3 m_s = -222$ MeV, -134 MeV, and without kaon condensation.

of gravitationally unstable sections in the mass – central density plot (see the black dashed curve), which have also been observed in Refs. [5, 9]. However, we consider this combination of extreme parameter choices unlikely, as it requires a very large density jump in the Maxwell construction (thus obliterating the soft part of the EOS) and also leads to unrealistically high central densities of the star. Furthermore, the case of a strong kaon condensate seems to be excluded in the present model now, as discussed before.

The global properties of the different configurations of (P)NS are summarized in Table II. One notes that the theoretical predictions for the maximum masses depend most importantly on the nuclear EOS, whereas the effects of kaon condensation and/or neutrino trapping are of smaller magnitude. Current observational values [48] suggest the existence of stars heavier than about $1.7 M_\odot$, although their accurate confirmation is still eagerly awaited. Even if they are, somewhat higher values of about $2 M_\odot$ would be required in order

to really discriminate between different nuclear EOS.

TABLE II: Properties of (proto)neutron stars.

	$a_3 m_s$ (MeV)	micro TBF		pheno TBF	
		M_{\max}/M_\odot	ρ_c/ρ_0	M_{\max}/M_\odot	ρ_c/ρ_0
trapped	—	2.19	6.29	1.80	8.24
$T = 30$ MeV	-134	2.14	6.24	1.75	7.82
	-222	2.05	7.12	1.61	11.47
untrapped	—	2.26	6.00	1.87	7.94
$T = 30$ MeV	-134	2.10	6.76	1.62	11.17
	-222	2.02	8.35	1.67	12.53
untrapped	—	2.34	6.29	1.92	8.76
$T = 0$	-134	2.11	6.88	1.62	11.76
	-222	2.03	8.47	1.70	12.94

V. SUMMARY

In conclusion, we presented microscopic calculations and convenient parametrizations of the equation of state of hot asymmetric nuclear matter within the framework of the Brueckner-Hartree-Fock approach with two different nuclear three-body forces. We then investigated the EOS as well as the consequences of including kaon condensation in hot and neutrino-trapped NS matter, employing a standard chiral model at finite temperature. Effects of finite temperature are thus included consistently in both the nucleonic and the kaonic part of the interaction.

Our results are qualitatively in agreement with those obtained with more phenomenological approaches [8, 9], although the quantitative predictions turn out to be different. In particular we found that also in our microscopic approach finite temperature plays a minor role compared to neutrino trapping, which generally decreases the stellar maximum mass in the absence of a kaon condensate, and increases it with a condensate. This is due to the reduced appearance of kaons in trapped vs. untrapped matter. Global PNS properties are, however, determined primarily by the *nucleonic* part of the EOS.

Furthermore, if recent very small values for the strangeness content of the proton are confirmed, kaon condensation in the present model sets in only at a critical density $\rho_c^K \gtrsim 4\rho_0$, whereas in the same BHF framework hyperons appear at $\rho_c^Y \approx (2-3)\rho_0$ [36, 39, 49], and would then completely suppress the kaon degree of freedom. In any case, the maximum mass of a (P)NS is strongly reduced by the appearance of strangeness in the relevant dense environment, either in the form of kaons, or of hyperons; and, in both cases a delayed collapse scenario appears very probable.

Acknowledgments

This work is supported in part by the National Natural Science Foundation of China (10605018,10905048,10975116), the Knowledge Innovation Project (KJ CX3-SYW-N2) of the Chinese Academy of Sciences, the Program for New Century Excellent Talents in University (NCET-07-0730), the Asia-Europe Link project (CN/ASIA-LINK/008(94791)) of the European Commission, and by COMPSTAR, a research networking program of the European Science Foundation.

-
- [1] D. B. Kaplan and A. E. Nelson, Phys. Lett. **B175**, 57 (1986); Nucl. Phys. **A479**, 273 (1988).
 - [2] H. D. Politzer and M. B. Wise, Phys. Lett. **B273**, 156 (1991).
 - [3] G. E. Brown, K. Kubodera, M. Rho, and V. Thorsson, Phys. Lett. **B291**, 355 (1992).
 - [4] C. H. Lee, G. E. Brown, D. P. Min, and M. Rho, Nucl. Phys. **A585**, 401 (1995); C. H. Lee, Phys. Rep. **275**, 255 (1996) and references therein; G. E. Brown, C. H. Lee, and M. Rho, Phys. Rep. **462**, 1 (2008).
 - [5] V. Thorsson, M. Prakash, and J. M. Lattimer, Nucl. Phys. **A572**, 693 (1994); **A574**, 851 (1994), Erratum.
 - [6] P. J. Ellis, R. Knorren, and M. Prakash, Phys. Lett. **B349**, 11 (1995).
 - [7] N. K. Glendenning and J. Schaffner-Bielich, Phys. Rev. Lett. **81**, 4564 (1998); Phys. Rev. **C60**, 025803 (1999).
 - [8] M. Prakash, I. Bombaci, M. Prakash, P. J. Ellis, J. M. Lattimer, and R. Knorren, Phys. Rep. **280**, 1 (1997).
 - [9] T. Tatsumi and M. Yasuhira, Phys. Lett. **B441**, 9 (1998); Nucl. Phys. **A653**, 133 (1999); M. Yasuhira and T. Tatsumi, Nucl. Phys. **A690**, 769 (2001); T. Muto, M. Yasuhira, T. Tatsumi, and N. Iwamoto, Phys. Rev. **D67**, 103002 (2003).
 - [10] T. Muto, T. Tatsumi, and N. Iwamoto, Phys. Rev. **D61**, 063001,083002 (2000).
 - [11] J. A. Pons, S. Reddy, P. J. Ellis, M. Prakash, and J. M. Lattimer, Phys. Rev. **C62**, 035803 (2000); J. A. Pons, J. A. Miralles, M. Prakash, and J. M. Lattimer, Astrophys. J. **553**, 382 (2001).
 - [12] A. Ramos, J. S. Bielich, and J. Wambach, Lect. Notes. Phys. **578**, 175 (2001).
 - [13] J. Carlson, H. Heiselberg, and V. R. Pandharipande, Phys. Rev. **C63**, 017603 (2000).
 - [14] T. Norsen and S. Reddy, Phys. Rev. **C63**, 065804 (2001).
 - [15] S. Kubis and M. Kutschera, Nucl. Phys. **A720**, 189 (2003).
 - [16] W. Zuo, A. Li, Z. H. Li, and U. Lombardo, Phys. Rev. **C70**, 055802 (2004).
 - [17] A. Li, G. F. Burgio, U. Lombardo, and W. Zuo, Phys. Rev. **C74**, 055801 (2006).
 - [18] M. Fukugita, Y. Kuramashi, M. Okawa, and A. Ukawa, Phys. Rev. **D51**, 5319 (1995).
 - [19] S. J. Dong, J.-F. Lagaë, and K. F. Liu, Phys. Rev. **D54**, 5496 (1996).
 - [20] S. Güsken et al., Phys. Rev. **D59**, 054504 (1999).
 - [21] V. E. Lyubovitskij, T. Gutsche, A. Faessler, and E. G. Drukarev, Phys. Rev. **D63**, 054026 (2001).
 - [22] H. Ohki et al., Phys. Rev. **D78**, 054502 (2008).
 - [23] R. Knorren, M. Prakash, and P. J. Ellis, Phys. Rev. **C52**, 3470 (1995); J. Schaffner-Bielich and I. N. Mishustin, Phys. Rev. **C53**, 1416 (1996); T. Muto, Phys. Rev. **C77**, 015810 (2008).
 - [24] T. W. Baumgarte, S. L. Shapiro, and S. A. Teukolsky, Ap. J. **458**, 680 (1996).
 - [25] T. Takatsuka, Prog. Theor. Phys. **95**, 901 (1996).
 - [26] K. Strobel, C. Schaab, M. K. Weigel, Astron. Astrophys., **350**, 497 (1999); K. Strobel, M. K. Weigel, Astron. Astrophys., **367**, 582 (2001).
 - [27] O. E. Nicotra, M. Baldo, G. F. Burgio, and H.-J. Schulze, Astron. Astrophys. **451**, 213 (2006); O. E. Nicotra, M. Baldo, G. F. Burgio, and H.-J. Schulze, Phys. Rev. **D74**, 123001 (2006).
 - [28] G. F. Burgio and H.-J. Schulze, Physics of Atomic Nuclei **72**, 1197 (2009).
 - [29] A. Lejeune, P. Grangé, M. Martzloff, and J. Cugnon, Nucl. Phys. **A453**, 189 (1986).
 - [30] I. Bombaci and U. Lombardo, Phys. Rev. **C44**, 1892 (1991); W. Zuo, I. Bombaci, and U. Lombardo, Phys. Rev. **C60**, 024605 (1999).
 - [31] M. Baldo, *Nuclear Methods and the Nuclear Equation of State*, International Review of Nuclear Physics, Vol. 8 (World Scientific, Singapore, 1999).
 - [32] M. Baldo and L. S. Ferreira, Phys. Rev. **C59**, 682 (1999).
 - [33] R. B. Wiringa, V. G. J. Stoks, and R. Schiavilla, Phys. Rev. **C51**,

- 38 (1995).
- [34] P. Grangé, A. Lejeune, M. Martzloff, and J.-F. Mathiot, *Phys. Rev.* **C40**, 1040 (1989).
- [35] W. Zuo, A. Lejeune, U. Lombardo, and J.-F. Mathiot, *Nucl. Phys.* **A706**, 418 (2002); Z. H. Li, U. Lombardo, H.-J. Schulze, and W. Zuo, *Phys. Rev.* **C77**, 034316 (2008).
- [36] Z. H. Li and H.-J. Schulze, *Phys. Rev.* **C78**, 028801 (2008).
- [37] J. Carlson, V. R. Pandharipande, and R. B. Wiringa, *Nucl. Phys.* **A401**, 59 (1983); R. Schiavilla, V. R. Pandharipande, and R. B. Wiringa, *Nucl. Phys.* **A449**, 219 (1986).
- [38] M. Baldo, I. Bombaci, and G. F. Burgio, *Astron. Astrophys.* **328**, 274 (1997); X. R. Zhou, G. F. Burgio, U. Lombardo, H.-J. Schulze, and W. Zuo, *Phys. Rev.* **C69**, 018801 (2004).
- [39] M. Baldo, G. F. Burgio, and H.-J. Schulze, *Phys. Rev.* **C58**, 3688 (1998).
- [40] S. L. Shapiro and S. A. Teukolsky, *Black Holes, White Dwarfs, and Neutron Stars* (John Wiley and Sons, New York, 1983).
- [41] A. Burrows and J. M. Lattimer, *Astrophys. J.* **307**, 178 (1986).
- [42] J. A. Pons, S. Reddy, M. Prakash, J. M. Lattimer, and J. A. Miralles, *Astrophys. J.* **513**, 780 (1999); L. Villain, J. A. Pons, P. Cerdá-Durán, and E. Gourgoulhon, *Astron. Astrophys.* **418**, 283 (2004).
- [43] J. W. Negele and D. Vautherin, *Nucl. Phys.* **A207**, 298 (1973).
- [44] G. Baym, C. Pethick, and D. Sutherland, *Astrophys. J.* **170**, 299 (1971).
- [45] R. Feynman, F. Metropolis, and E. Teller, *Phys. Rev.* **C75**, 1561 (1949).
- [46] D. Gondek, P. Haensel, and J. L. Zdunik, *Astron. Astrophys.* **325**, 217 (1997).
- [47] A. B. Migdal, in *Mesons in Nuclei*, vol. 3, eds. M. Rho and D. Wilkinson (North-Holland, Amsterdam, 1979).
- [48] J. M. Lattimer and M. Prakash, *Phys. Rep.* **442**, 109 (2007).
- [49] M. Baldo, G. F. Burgio, and H.-J. Schulze, *Phys. Rev.* **C61**, 055801 (2000); H.-J. Schulze, A. Polls, A. Ramos, and I. Vidaña, *Phys. Rev.* **C73**, 058801 (2006).